Aliphatic Polyurethane–Montmorillonite Nanocomposite Coatings: Preparation, Characterization, and Anticorrosive Properties

Shabnam Ashhari, Ali Asghar Sarabi, Seyed Mahmoud Kasiriha, Davood Zaarei

Polymer Faculty, Amirkabir University of Technology, P.O. Box 15875, Tehran, Iran

Received 2 February 2010; accepted 15 April 2010
DOI 10.1002/app.32656
Published online 27 July 2010 in Wiley Online Library (wileyonlinelibrary.com).

ABSTRACT: Polyurethane (PU)–clay nanocomposite coatings were prepared by a sonication method. The stability and morphology of these coatings was characterized by turbidometry, X-ray diffraction, and transmission electron microscopy. The anticorrosive properties of these coatings were investigated by salt-spray and electrochemical impedance spectroscopy methods. According to the results, dispersed nanoclay layers in the matrix of the nanocomposite coating compositions led to superior anticorrosive characteristics compared to those of pure PU coatings. The best results were obtained with coatings containing about 5 wt % clay. The resistance of the coating containing 5% clay was about 9.002 GΩ after 225 days of immersion in a 3.5 wt % NaCl solution, whereas it was only 97 kΩ for the pure PU coating. © 2010 Wiley Periodicals, Inc. J Appl Polym Sci 119: 523–529, 2011

Key words: barrier; clay; coatings

INTRODUCTION

Polymer nanocomposites have received significant attention in recent years because they lead to improved physical and chemical properties and often exhibit superior characteristics in comparison with pure polymers.[1,2]

The results of research done on nanocomposites has shown that nanoclay particles have a significant effect on improving the thermal, mechanical, and gas-barrier properties of the nanocomposites in comparison with pure polymers, even in the presence of very small amounts of these modified nanoparticles.[3–6] Polymer–clay nanocomposite coatings have gained increasing attention in both academia and industry. Various articles have been published on new methods for the preparation of different kinds of polymeric matrices, such as polyurethane (PU)–clay nanocomposites.[4,7–10]

Montmorillonite (MMT) is a special type of layered silicate,[1,11–13] which has been used for the preparation of polymer–clay nanocomposites because of its lamellar structure. MMT can improve some properties, such as the stiffness and barrier properties, of MMT–polymer nanocomposites coatings in comparison to pure polymeric coatings.[4]

To achieve the best properties of polymer–clay nanocomposites, the important factor is to obtain a stable dispersion in which the silicate nanolayers are completely exfoliated in the polymeric matrix;[14–18] therefore, during nanocomposite preparation, the evaluation and assessment of the morphology of these nanocomposites is very important.

Aliphatic PU coatings have been used as topcoats and one-coat finishes because of their good resistance to weathering, chemicals, and yellowing.[19] Hexamethylene diisocyanate (HDI) is a common hardener for preparing aliphatic PUs. HDI reacts with a polyol at low temperatures and produces aliphatic PU coatings with good properties.[20] There are several studies on the preparation of PU–clay nanocomposites,[4,7–10] but to our knowledge, no research has thus far been done on the preparation of aliphatic PU–clay nanocomposite coatings.

In this study, modified nanoclay was dispersed into an aliphatic PU matrix via a sonication method. The prepared nanocomposites were applied on carbon steel panels. The morphology of these coatings was characterized by X-ray diffraction (XRD), transmission electron microscopy (TEM), and turbidometry. The anticorrosive properties of these coatings were studied by electrochemical impedance spectroscopy (EIS) measurements on the coated steel panels after 225 days of immersion in a 3.5 wt % NaCl solution.

EXPERIMENTAL

Materials

The nanoclay used in this study was a modified MMT of the commercial brand Cloisite 30B (C30B),

Correspondence to: A. A. Sarabi (sarabi@aut.ac.ir).

TABLE I
Acrylic Polyol Specifications

Type	Solvent	NV (%)	Acid value
Acrylic polyol	Xylene	49–51	<15

manufactured by Southern Clay Products. Acrylic polyol (non volatile content (NV) = 59–61 wt %, acid value < 5) was purchased from Hitech Co. (Dubai, United Arab Emirates) with the specifications given in Table I, and HDI (solid content ≈ 75 wt %) was produced by Bayer Co. (Leverkusen, Germany), with the technical data shown in Table II.

Sample preparation

For the preparation of the compositions, first, the polyol resin was slowly heated to 50°C, and then, the desired amount of organoclay was gradually poured into the resin with stirring. To decrease the viscosity and ease mixing, the mixtures were held at 70–80°C and stirred at 2500 rpm for 2.5 h with a high-shear mixer. For degassing, the samples were held in a vacuum oven at 70–75°C for 30 min, and the foam of tiny bubbles were removed. After high-shear mixing, samples of these mixed compositions containing organoclay and polyol were sonicated with a high-powered sonication instrument (UP 400S, Heischler Co., Teltow, Germany) for 20 min. During ultrasonication, we gradually raised the power of sonication while maintaining the temperature of the mixtures at 20–25°C by placing the reaction vessels in a cool-water jacket. The sonicated compositions containing 0, 1, 3, 5, and 7 wt % C30B were known as PU, PU–MMT1, PU–MMT3, PU–MMT5, and PU–MMT7, respectively.

Surface preparation of the steel panels and application of the coating

The steel panels first were degreased chemically by acetone and were then polished mechanically with 600, 800, and 1000 emery papers. The stoichiometric amount of the hardener, HDI, was added to the base components (polyol-containing nanoparticles). The mixtures were applied by a film applicator on steel panels. During the application process, the coating compositions containing up to 5 wt % of organoclay clay showed nice flow and good leveling.

After curing, the dry film thicknesses were 40 ± 2 μm. For better judgment and evaluation of the reliability, five panels were coated by each coating composition.

Characterizations of the PU–clay nanocomposites

Turbidometry

We evaluated the stability of the samples by measuring the turbidity of the samples at different time intervals by using a turbidometer 2100 A by Hatch Co. (Loveland, United States)

XRD

This analysis was carried out with a Philips model X'PERT MPD X-ray diffractometer with Cu Kα radiation (λ = 1.5401 Å) operating at 40 kV and 40 mA for determining the interlayer distance of the clay particles in the polymeric matrix. Diffraction patterns were obtained in the 2θ range 0.5–10° at a rate of 1°/min; the step size was 0.02.

TEM

This technique was used to analyze the morphology of the bulk samples and to evaluate the state of dispersion. The TEM samples were prepared by cutting the cured bulk nanocomposites by an ultramicrotome instrument (OMU3, Reichert, Vienna, Austria) that was equipped with a diamond cutter. The thickness of the TEM samples was about 70–100 nm. Then, the samples were put on 300-mesh copper grids. Transmission electron micrographs were taken with a Philips-CM200 (Amsterdam, The Netherlands) at an acceleration voltage of 200 kV.

Corrosion tests

Salt spray

This test was used to evaluate performance of the PU–clay nanocomposite coatings by standard methods.[21,22] The salt-spray instrument used was CST-114 (Biazma Co., Esfehan, Iran).

EIS

Impedance measurements were carried out in a three-electrode system made by Ivium Compactstat (Eindhoven, The Netherlands). A saturated calomel electrode and graphite rod were used as a reference electrode and auxiliary electrode, respectively. About 1 cm^2 of the coated metals was exposed to 3.5 wt % NaCl electrolyte, and the rest was covered with a 75/25 beeswax–colophony mixture. The frequency range used was 100 kHz to 10 mHz, and the perturbation was 10 mV. The software used for determining the

TABLE II
HDI Specifications

Property	Value
NCO content (%)	16.5 ± 0.3
Viscosity at 25°C (mPa s)	150 ± 60
Monomeric HDI (%)	0.5 maximum
Solids (%)	75 ± 1

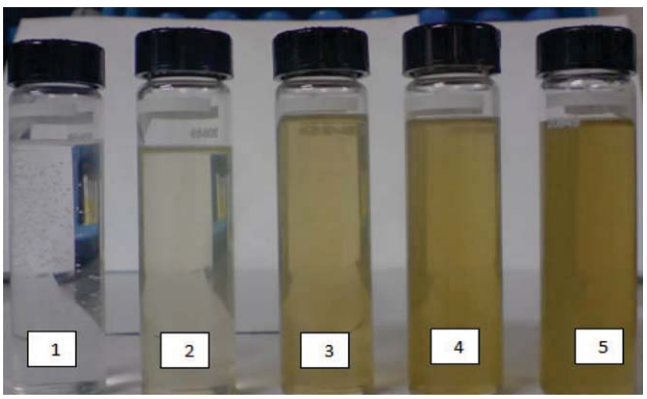

Figure 1 Cells of the turbidometer containing (1) PU, (2) PU–MMT1, (3) PU–MMT5, (4) PU–MMT7, and (5) PU–MMT7. [Color figure can be viewed in the online issue, which is available at wileyonlinelibrary.com.]

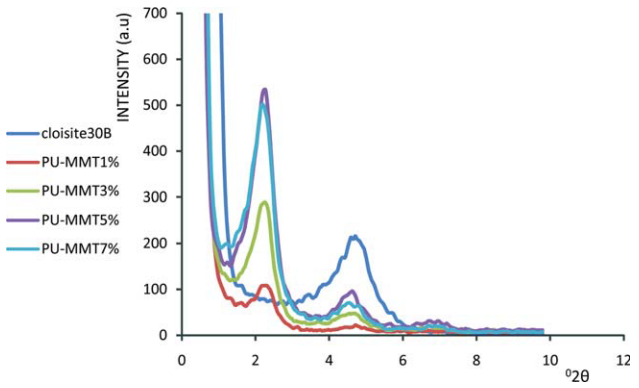

Figure 2 XRD patterns of the PU–MMT nanocomposites: (a) MMT, (b) PU–MMT1, (c) PU–MMT3, (d) PU–MMT5, and (e) PU–MMT7. [Color figure can be viewed in the online issue, which is available at wileyonlinelibrary.com.]

equivalent circuit and data analysis was Ivium Equivalent Circuit Evaluator (Eindhoven, The Netherlands).

RESULTS AND DISCUSSION

Test results

Turbidity results

Figure 1 shows the turbidometer's cells containing PU, PU–MMT1, PU–MMT3, PU–MMT5, and PU–MMT7 samples. The turbidity results at different time intervals are shown in Table III.

However, the reduction of turbidity over time indicated the increment of sample clarity and also the reduction of particles, which dispersed in the media. On the other hand, the reduction of particles over a long period of time in the resinous media indicated the aggregation and sedimentation of the particles and also a weakness of dispersion. With attention to the result of turbidometry and the negligible changes in turbidity in all of the samples, we concluded that the dispersions were stable and that no sedimentation occurred during the test.

XRD results

XRD analysis was carried out to measure the space between the silicate layers of the clay particles before and after dispersion in the polymeric matrix. The XRD patterns of the PU–MMT compositions are presented in Figure 2. On the basis of Braggs law, d_{001} (distance between silicate layers) of C30B was 18.02 Å, and a broad peak for the entire PU–MMT nanocomposite was observed at $2\theta = 2.184°$; this revealed that the layered silicates of MMT were intercalated to a space of 44.128 Å by the PU polymer chains.

As depicted in Figure 2, the 2θ values for all of the nanocomposite samples showed a peak near 2.5°, which meant that d_{001} for these samples was about 40–45 Å. On the other hand, 2θ for the C30B powder sample showed a peak near 4.3°, which meant that d_{001} for these samples was about 18.02 Å. The difference between the d_{001} values of the C30B powder and nanocomposite samples was between 22 and 27 Å; this indicated that the penetration of polyol into the clay galleries and intercalation occurred.

TEM results

Figure 3 shows TEM images of the PU–MMT5 sample with two different magnifications, where the dark areas show clay platelets and the gray areas represent the polymeric matrix. Figure 3(a) is a lower magnification micrograph, and Figure 3(b) is a high-magnification micrograph. The dominant morphology was intercalation. The main reason for this

TABLE III
Results of the Turbidity Measurements at Different Times

Sample code	NTU after 20 h	NTU after 24 h	NTU after 27 h	NTU after 47 h	NTU after 51 h	NTU after 219 h
PU	0.876	0.876	0.876	0.876	0.876	0.876
PU–MMT1%	36.3	35.4	35.1	34.8	34.6	34.6
PU–MMT3%	101	100	99.4	97.8	97.2	96.6
PU–MMT5%	168	163	163	163	161	160.1
PU–MMT7%	260	258	256	252	252	250

NTU, nephelometric turbidity units

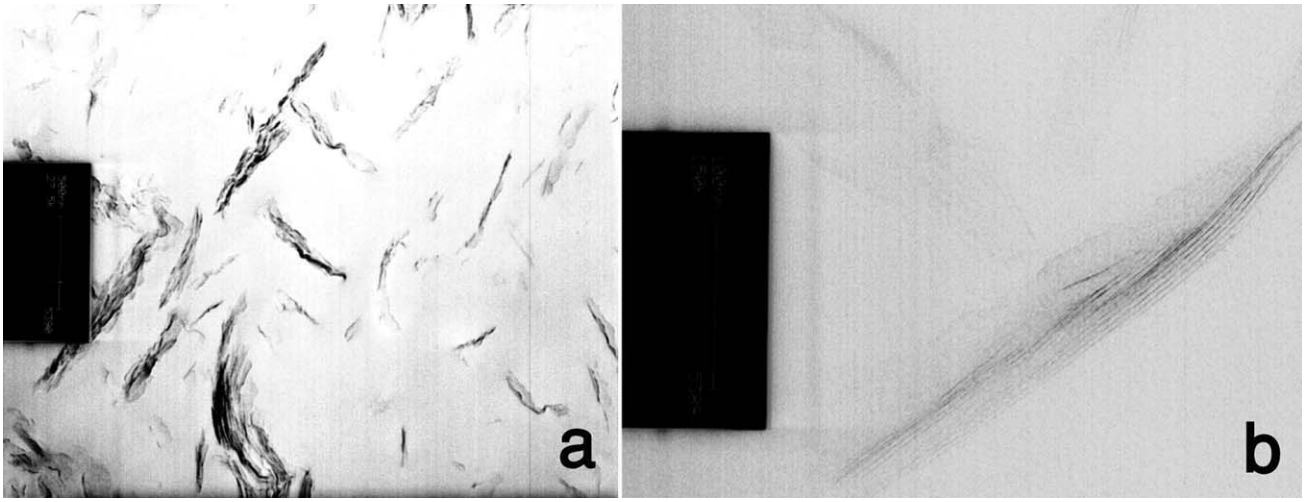

Figure 3 TEM of PU–MMT5 with (a) 27.5 and (b) 150× magnification.

morphology was the method of nanocomposite preparation.[23] The morphology played an important role in the properties of the final nanocomposite.[14,15] On the basis of the TEM results, we concluded that our used method for nanocomposite preparation (high-shear mixing and sonication) was an acceptable method for the reduction of the stacks and the introduction of resin into the galleries of the clays.

The results of the turbidometry, XRD, and TEM analyses confirmed each other and indicated that the dispersion of silicate layers into the polymeric matrix occurred.

Salt-spray results

Table IV shows the results of the salt-spray tests of the nanocomposites and pure coating after 408 h of exposure to the 5 wt % NaCl media. According to Table IV, increasing the amount of nanoclay particles in the matrix led to the reduction of the blistering density of the resulting coatings. The main reason for this was the platelike structure of the clay particles, which increased the coating's barrier properties.[24–27] This means that for the nanocomposite coatings containing 5 wt % clay or greater, the corrosion of substrates occurred with a long time delay because the tortuosity that was formed by these nanoparticles increased the way that the corrosive ions needed to reach to the substrate.[28]

TABLE IV
Salt-Spray Results of the PU–Clay Nanocomposites with Various Clay Contents in Accordance with ASTM D 714 and ASTM B117

Clay concentration (wt %)	Results
0	A lot of blisters were observed on the surface (blister size no. 6, medium). There was a trace of rust under the blisters.
1	A lot of small blisters were observed on the surface (blister size no. 8, medium). There was a trace of rust under the blisters.
3	There was a small amount of blisters on the surface (blister 3%, size no. 8, few).
5	There was no blister and water penetration.
7	There was no blister and water penetration.

EIS results

The corrosion-protection properties of the PU–clay nanocomposites coated on steel were evaluated by

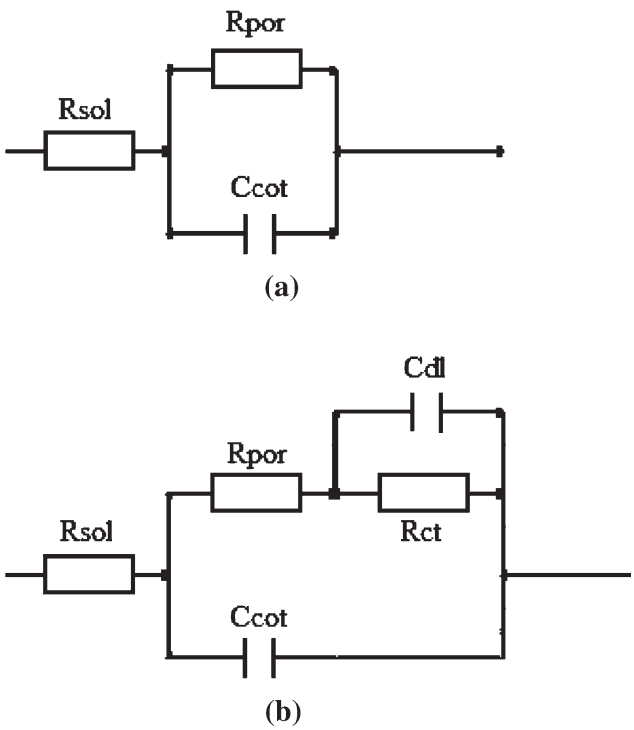

Figure 4 Equivalent circuits used to simulate the results of the EIS tests.

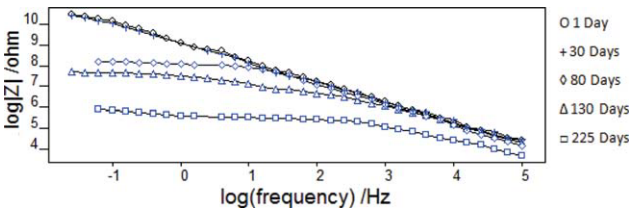

Figure 5 Bode plot of the PU sample after different immersion times in a 3.5 wt % NaCl solution. [Color figure can be viewed in the online issue, which is available at wileyonlinelibrary.com.]

the coating resistance (R_{por}) values during different times of immersion in a 3.5 wt % NaCl solution. These results we obtained from Bode diagrams and the equivalent circuits, which are shown in Figure 4. In these circuits, R_{sol}, R_{por}, and C_{coat} were resistance of the electrolyte, pore resistance, and capacitance of the coating, respectively. The circuit shown in Figure 4(a) was used to fit the EIS diagrams of samples with high resistance, and the circuit shown in

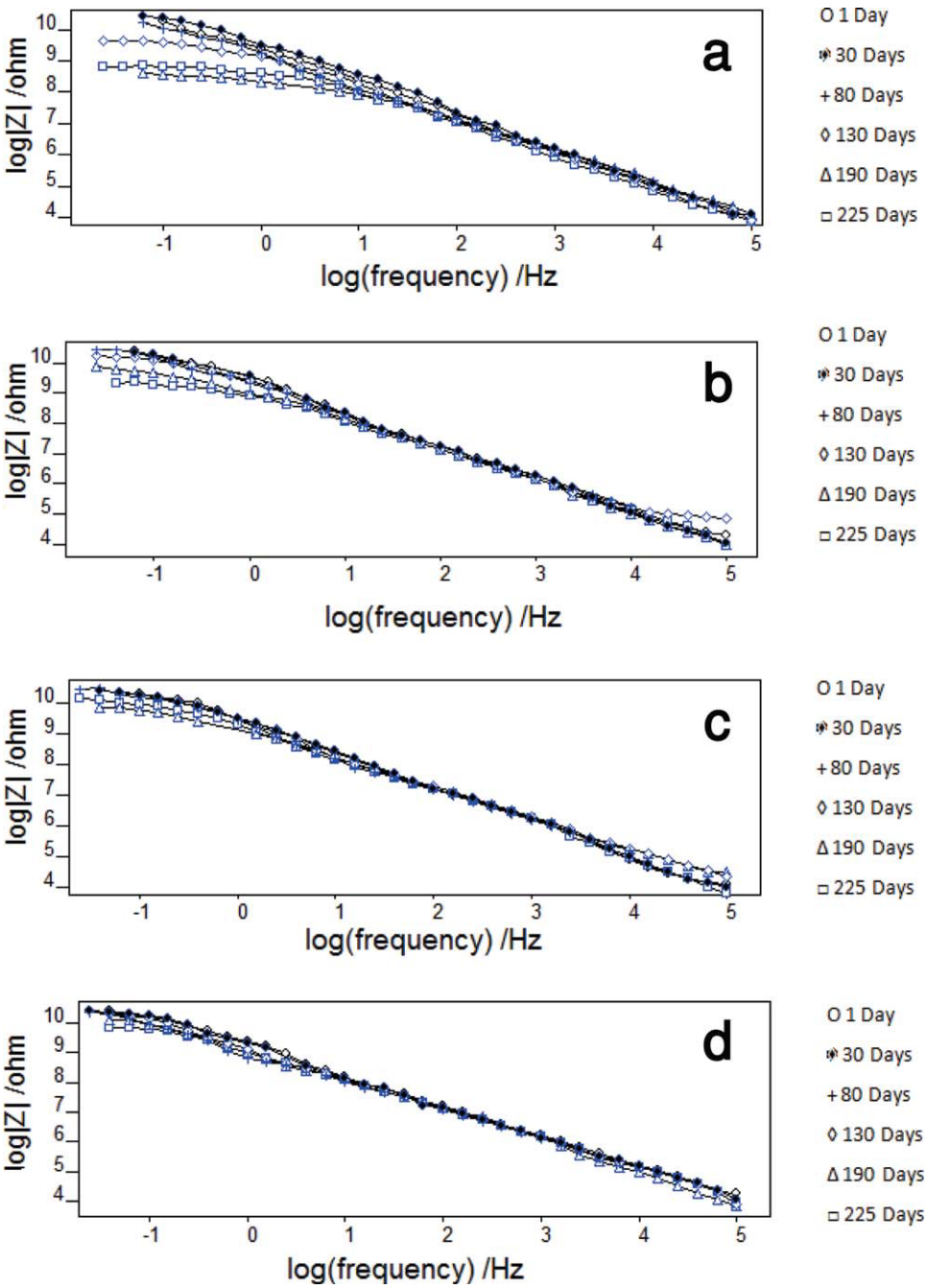

Figure 6 Bode plots of (a) PU–MMT1, (b) PU–MMT3, (c) PU–MMT5, and (d) PU–MMT7 at different immersion times in a 3.5 wt % NaCl solution. [Color figure can be viewed in the online issue, which is available at wileyonlinelibrary.com.]

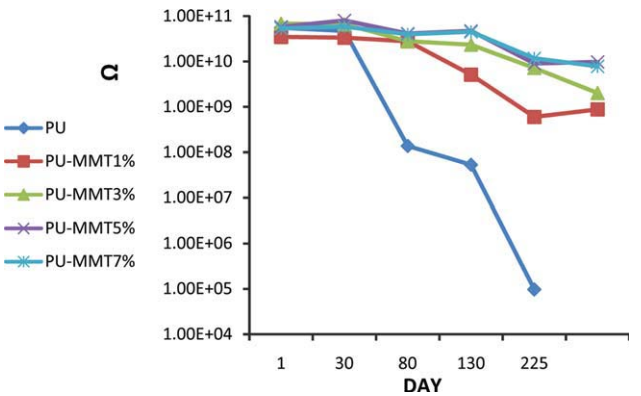

Figure 7 Pore resistance of PU and the PU–MMT nanocomposites at different immersion times in a 3.5 wt % NaCl. [Color figure can be viewed in the online issue, which is available at wileyonlinelibrary.com.]

Figure 4(b) was used to fit the low-resistance coatings' EIS diagrams.

The Bode plots of samples during 225 days of immersion in 3.5 wt % NaCl solution are shown in Figures 5 and 6. Comparing the Bode plots, we observed that over a long period of immersion time, the PU–MMT5 and PU–MMT7 samples showed the highest impedance modulus at low frequencies. This means that the highest protection of steel was accrued by these nanocomposite coatings. Nanoparticles with a platelike structure can make a barrier layer in the polymeric matrix, which can prevent the penetration of electrolyte through the coating and, consequently, prevent the corrosion by barrier mechanism;[1,29] also, their nanosize increases the tortuosity of the penetration path of corrosive ions, which will cause a delay in the corrosion process.

As shown in Figure 7, the addition of organoclay into the PU coating causes an increase in the pore resistance during the long period of immersion in 3.5 wt % NaCl solution. Higher values of R_{por} mean higher corrosion protection and lower ion permeability through the coating.[30] Among the nanocomposite samples, after 225 days of immersion, PU–MMT5 and PU–MMT7 showed the highest R_{por}, so the PU–MMT5 and PU–MMT7 films had the highest anticorrosive protection on the metal surfaces. The increase in the R_{por} values of PU–MMT nanocomposites is because of the incorporation of clay into the polymer matrix, which decreased corrosive-ion permeability through the formation of tortuosities. The ion permeability depended on length, orientation, and degree of delamination of layered silicates.[31] As the dispersion and delamination of clay layers were observed in the TEM and XRD patterns, better corrosion protection, due to the blocking of the pores and defects of these coatings, was predictable.[32,33] As shown in Figure 7, the PU–MMT5 and PU–MMT7 samples had a high pore resistance and good performance. On the other hand, because of the ease of application, leveling, and economic problems, PU–MMT5 is preferred for use.

CONCLUSIONS

PU–clay nanocomposite coatings were prepared the dispersion of modified MMT clay into the PU matrix via a sonication method. The results of XRD, TEM, and optical microscopy analyses of the cured nanocomposites indicated that the clay particles were dispersed and intercalated into the PU polymers. In addition, the results of a series of electrochemical measurements indicate that the PU–clay nanocomposite films showed a greater corrosion protection effect on the steel surfaces than the pure PU film over 225 days of immersion in the 3.5 wt % aqueous NaCl solution. The metals coated by the nanocomposites containing 5 and 7 wt % MMT clay showed the highest corrosion resistance. The good corrosion-protection effects of these coatings were due to the well-dispersed and intercalated nanoparticles in the PU matrix.

References

1. Pinnavaia, T. J.; Beall, G. W. Polymer–Clay Nanocomposites; Wiley Series in Polymer Science; Wiley: New York, 2000.
2. Meneghetti, P.; Qutubuddin, S. J Thermochim Acta 2006, 442, 74.
3. Yeh, J. M.; Huang, H. Y.; Chen, C. L.; Su, W. F.; Yu, Y. H. Surf Coat Technol 2006, 200, 2753.
4. Zaarei, D.; Sarabi, A. A.; Sharif, F.; Kassiriha, S. M. JCT Res 2008, 5, 241.
5. Yu, Y. H.; Yeh, J. M.; Liou, S. J.; Chen, C. L.; Liaw, D. J.; Lu, H. Y. J Appl Polym Sci 2004, 92, 3573.
6. Ke, Y. C.; Strove, P. Polymer Layered Silicate and Silica Nanocomposites; Elsevier: Amsterdam, 2005.
7. Chen-Yang, Y.; Yang, H.; Li, G.; Li, Y. J Polym Res 2005, 11, 275.
8. Mondal, P.; Khakhar, D. V. J Appl Polym Sci 2007, 103, 2802.
9. Lee, H. T.; Lin, L. H. Macromolecules 2006, 39, 6133.
10. Ni, P.; Li, J.; Suo, J.; Li, S. J Appl Polym Sci 2004, 94, 534.
11. Zhang, Z.; Sparks, D. L.; Scrivner, N. C. J Environ Sci Technol 1993, 27, 1625.
12. Blumstein, A. J Polym Sci Part A: Gen Pap 1965, 3, 2665.
13. Theng, B. K. G. Formation and Properties of Clay—Polymer Complexes; Elsevier: Amsterdam, 1979.
14. Giannelis, E. P. J. Adv Mater 1996, 8, 29.
15. Fornes, T. D.; Yoon, P. J.; Keskkula, H.; Paul, D. R. Polymer 2001, 42, 09929.
16. Samyn, F.; Bourbigot, S.; Jama, C.; Bellayer, S.; Nazare, S.; Hull, R.; Castrovinci, A.; Fina, A.; Camino, G. Eur Polym J 2008, 44, 1642.
17. Ratna, D.; Divekar, S.; Samui, A. B.; Chakraborty, B. C.; Banthia, A. K. Polymer 2006, 47, 4068.
18. Wagener, R.; Reisinger, T. Polymer 2003, 44, 7513.
19. Bock, M. Polyurethane for Coatings; Vincentz Verlag: Hanover, Germany, 2001.
20. Li, S.; Vatanparast, R.; Lemmetyinen, H. Polymer 2000, 41, 5571.

21. In Book of Standards; ASTM B 117-09; American Society for Testing and Materials: West Conshohocken, PA; Vol.03.02, 2003.
22. In Book of Standards; ASTM D 714; American Society for Testing and Materials: West Conshohocken, PA; Volume: 06.01, 2003.
23. Malucelli, G.; Di Gianni, A.; Deflorian, F.; Fedel, M.; Bongiovanni, R. Corros Sci 2009, 51, 1762.
24. Thomassina, J. M.; Pagnoullea, C.; Caldarellab, G.; Germainb, A.; Jérômea, R. J Membr Sci 2006, 270, 50.
25. Okada, A.; Kawasumi, M.; Usuki, A.; Kojima, Y.; Kurauchi, T.; Kamigaito, O. Mater Res Soc Proc 1990, 171, 45.
26. Kojima, Y.; Usuki, A.; Kawashmi, M.; Okada, A.; Kurauchi, T.; Kamigalto, O. J Appl Polym Sci 1993, 49, 1259.
27. Messersmith, P. B.; Giannelis, E. P. J Appl Polym Sci Part A: 1995, 33, 1047.
28. Bharadwaj, R. K. Macromolecules. 2001, 34, 9189.
29. Mai, Y. W.; Yu, Z. Z. Polymer Nanocomposites; Woodhead: Cambridge, England, 2006.
30. Le Thua, Q.; Bierwagen, G. P.; Touzain, S. Prog Org Coat 2001, 42, 179.
31. Castela, A. S. L.; Simoes, A. M.; Ferreia, M. G. S. Prog Org Coat 2000, 38, 1.
32. Changa, K. C.; Lai, M. C.; Peng, C. W.; Chena, Y. T.; Yeh, J. M.; Lin, C. L.; Yang, J. C. J Electrochim Acta 2006, 51, 5645.
33. Yeh, J. M.; Kuo, T. H.; Huang, H. J.; Chang, K. C.; Chang, M. Y.; Yang, J. C. Eur Polym J 2007, 43, 1624.